

# A LOCAL DISCONTINUOUS GALERKIN METHOD FOR THE BENAJAMIN-ONO EQUATION

MUKUL DWIVEDI AND TANMAY SARKAR

**ABSTRACT.** The main purpose of this paper is to design a local discontinuous Galerkin (LDG) method for the Benjamin-Ono equation. We analyze the stability and error estimates for the semi-discrete LDG scheme. We prove that the scheme is  $L^2$ -stable and it converges at a rate  $\mathcal{O}(h^{k+1/2})$  for general nonlinear flux. Furthermore, we develop fully discrete LDG scheme using the Crank-Nicolson (CN) and fourth order fourth stage Runge-Kutta (RK) method in time. Adapting the methodology established for the semi-discrete scheme, we demonstrate the stability of the fully discrete CN-LDG scheme and derive an error estimate of an order of convergence  $\mathcal{O}(h^{k+1/2})$  for general nonlinear flux. Additionally, we prove that the RK-LDG scheme is strongly stable under an appropriate time step constraint by establishing a *three-step strong stability* estimate for linear flux. Numerical examples are provided to validate the efficiency and accuracy of the method.

## 1. INTRODUCTION

We consider the following Cauchy problem associated to generalized Benjamin-Ono (BO) equation:

$$\begin{cases} U_t + f(U)_x - \mathcal{H}U_{xx} = 0, & (x, t) \in \mathbb{R} \times (0, T], \\ U(x, 0) = U_0(x), & x \in \mathbb{R}, \end{cases} \quad (1.1)$$

where  $T > 0$  is fixed,  $U_0$  represents the prescribed initial data,  $f$  is any given function of  $U$  and  $U : \mathbb{R} \times (0, T] \rightarrow \mathbb{R}$  is the unknown, and  $\mathcal{H}$  denotes the Hilbert transform [12, 35], defined by the principle value integral

$$\mathcal{H}U(x) := \text{P.V.} \frac{1}{\pi} \int_{\mathbb{R}} \frac{U(x-y)}{y} dy.$$

The Benjamin-Ono equation (1.1) is a nonlinear, non-local partial differential equation that finds application in various physical phenomena [22, 27]. In particular, the propagation of weakly nonlinear internal long waves in a fluid with a thin region of stratification can be represented by the BO equation. Originating from the modeling of waves in shallow water, it offers insights into the behavior of these waves, including their propagation and interaction. Moreover, the BO equation emerges as a fundamental model in diverse fields such as fluid dynamics, nonlinear optics, and plasma physics, reflecting its broad relevance in understanding wave dynamics and nonlinear wave interactions. Furthermore, we mention that it defines a Hamiltonian system, and with the help of inverse scattering method (see [1]), families of localized solitary wave solutions, called as soliton solutions [8], can be obtained under the appropriate assumptions on the initial data. Since the BO equation is completely integrable, it admits infinitely many conserved quantities [8].

The investigation into the well-posedness of the Cauchy problem (1.1) associated to the BO equation has been the subject of extensive research over the years. Pioneering work in the local

---

(Mukul Dwivedi)

DEPARTMENT OF MATHEMATICS, INDIAN INSTITUTE OF TECHNOLOGY JAMMU, JAGTI, NH-44 BYPASS ROAD, POST OFFICE NAGROTA, JAMMU - 181221, INDIA

(Tanmay Sarkar)

DEPARTMENT OF MATHEMATICS, INDIAN INSTITUTE OF TECHNOLOGY JAMMU, JAGTI, NH-44 BYPASS ROAD, POST OFFICE NAGROTA, JAMMU - 181221, INDIA

*E-mail addresses:* 2020rma1031@iitjammu.ac.in, tanmay.sarkar@iitjammu.ac.in.

*2020 Mathematics Subject Classification.* Primary: 65M60, 35R09; Secondary: 65M12.

*Key words and phrases.* Local discontinuous Galerkin method, Benjamin-Ono equation, Hilbert transform.

well-posedness was conducted by Iório [21] for the initial data in  $H^s(\mathbb{R})$ ,  $s > 3/2$  and making use of the conserved quantities, the global well-posedness for data in  $H^s(\mathbb{R})$ ,  $s \geq 2$  is demonstrated. Afterwards, the local well-posedness result is improved by Ponce [29] for  $H^{3/2}(\mathbb{R})$  data along with the global result for any solution in  $H^s(\mathbb{R})$ ,  $s \geq 3/2$  by using the smoothing properties and energy estimates. Further improvements in the local well-posedness were given by Koch et al. [25] for data in  $H^s(\mathbb{R})$ ,  $s > 5/4$  and using the argument given in [25], Kenig et al. [23] extended the result for  $s > 9/8$ . Tao in [34] also obtained the global well-posedness in  $H^1(\mathbb{R})$  by introducing the Gauge transformation. The idea of Gauge transformation given in [34] was further improved by Burq et al. [5] to carry out the local well-posedness to  $H^s(\mathbb{R})$  for  $s > 1/4$  and by Kenig et al. [20] to extend the same to  $H^s(\mathbb{R})$  for  $s \geq 0$ . Molinet [28] has also obtained the global well-posedness for the periodic data in  $L^2(\mathbb{R})$ .

It is well-known that due to the effects of dispersion and nonlinear convection, finding a reliable method for the BO equation is quite challenging task. Nevertheless, recent decades have seen the development of various numerical methods to solve the equation (1.1), with only the pertinent literature referenced here. An implicit finite difference method introduced by Thomée et al. [35] utilizes the continuous Hilbert transform. More recently, Dutta et al. [12] demonstrated the convergence of the fully discrete Crank-Nicolson scheme, which includes the discrete Hilbert transform, and Galtung [16, 17] devised a convergent Crank-Nicolson Galerkin scheme.

The discontinuous Galerkin (DG) approach, a class of finite element methods, was first introduced by Reed and Hill [30] in the framework of neutron transport equation. It employs discontinuous piecewise polynomial spaces for approximating both the solution and test functions. While this method demands more computational resources due to the discontinuities at the interfaces, it offers flexibility in selecting fluxes at these interfaces, ensuring high accuracy and stability. Afterwards, a significant breakthrough emerged in DG methodology given by Cockburn et al., for details, we refer to [10] and references therein, where the DG method is applied to nonlinear conservation laws. In their approach, the space DG discretization is incorporated with the Runge-Kutta (RK) time discretization and hence this method is often called as the Runge-Kutta discontinuous Galerkin (RKDG) method. The RKDG method is highly parallelizable due to the local character of DG schemes and the explicit time discretization. Nevertheless, equations containing higher-order derivative terms may not be directly tackled using the DG method. In such instances, higher-order derivatives might introduce instability and inconsistency as emphasized in [18]. To address these issues, Bassi and Rebay [4] made substantial progress by adapting the RKDG method for compressible Navier-Stokes equations. In their approach, both the solution and its gradient are treated as independent variables, marking a notable stride in the evolution of DG methodology.

Cockburn and Shu in [11] introduced a generalization of the Bassi and Rebay method called the local discontinuous Galerkin (LDG) method, stands as a cornerstone in addressing intricate higher-order problems. The methodology revolves around the transformation of equations into first-order systems, achieved by introducing auxiliary variables to approximate lower derivatives. The term “local” in LDG underscores the provisional nature of these auxiliary variables, which can be locally eliminated. Success with LDG method relies on designing numerical fluxes at the interfaces. These fluxes must be chosen to ensure stability and allow for solving the extra variables locally. This method is tailored to handle these equations efficiently and accurately.

The LDG method has been developed to deal with equations that have higher-order derivative terms. For instance, Yan and Shu [43] devised a LDG method for KdV type equations, which have third-order spatial derivatives. They obtained the error estimates with order of convergence  $k + 1/2$  in the linear case. Afterwards, Xu and Shu [40, 41] studied nonlinear equations and observed that the LDG method still provides similar levels of accuracy and order of convergence. Furthermore, Xu and Shu [42] also expanded the LDG method to handle equations with fourth and fifth order spatial derivatives. Levy et al. [26] also worked on adapting the LDG method for equations with compactly supported traveling wave solutions appearing in nonlinear dispersive equations.

In more recent times, the LDG method has become popular for dealing with partial differential equations that involve the non-local operator. Xu and Hesthaven [38] came up with an LDG method that breaks down the fractional Laplacian of order  $\alpha$  ( $1 < \alpha < 2$ ) into second-order

derivatives and fractional integrals of order  $2 - \alpha$ . This method turned out to be very effective, giving the optimal rates of  $k + 1$  in the linear case and  $k + 1/2$  in the nonlinear setup. Similarly, Aboelenen [2] and Dwivedi et al. [15] developed a LDG method specifically designed for fractional Schrödinger-type equations and fractional Korteweg-de Vries equation respectively.

Research on developing fully discrete LDG schemes with stability analysis and error estimation for equations involving higher-order derivatives without diffusion is quite limited. However, several studies have addressed fully discrete LDG schemes for equations which include diffusion terms, achieving both stability analysis and optimal error estimates. For instance, [36, 37] successfully established optimal error estimates using an implicit-explicit third-order RK-LDG method. Recent advancements have introduced a stable fully discrete LDG method known as the high-order RK-LDG method. Various studies have investigated the stability and accuracy of this method in various contexts, as seen in [31, 32, 33]. Recently, Hunter et al. [19] determined the stability of a fully discrete implicit-explicit RK method for the linearized KdV equation with periodic initial data using the Fourier method. Furthermore, Ai et al. [3] derived error estimates for the fully discrete RK-LDG method designed to solve scalar nonlinear conservation laws using the generalized Gauss-Radau projection. However, to the best of our knowledge, an LDG method has not yet been developed for the Benjamin-Ono equation.

In this paper, our approach to design the LDG scheme for the BO equation (1.1) involves introduction of auxiliary variables to represent (1.1) into the system of lower order derivatives. Since the BO equation (1.1) includes a non-local operator, the original problem is defined over the entire real line. However, for numerical methods, we limit the problem to a sufficiently large bounded domain and the solution having compact support within it. To design the scheme, we use the standard DG method within each element to all the equations of system of lower order derivatives. A crucial part of this process involves constructing appropriate numerical fluxes at the interior interfaces, while boundary numerical fluxes are determined by the provided boundary conditions. Additionally, to develop a fully discrete LDG scheme, we discretize time using the Crank-Nicolson method. We demonstrate that the fully discrete scheme is stable and derive error estimates for any general nonlinear flux. The main ingredients of the paper are enlisted below:

- (1) We design a LDG scheme for the BO equation (1.1) and establish the stability of the devised semi-discrete scheme with a general nonlinear flux. The stability analysis has also been extended for fully-discrete Crank-Nicolson scheme.
- (2) We also carry out the convergence analysis of the semi-discrete scheme and fully discrete Crank-Nicolson scheme. We obtain a convergence rate of  $\mathcal{O}(h^{k+1/2})$  considering any general nonlinear flux.
- (3) Furthermore, we extend our methodology to include higher order temporal discretization of equation (1.1) using the classical four-stage fourth-order Runge-Kutta (RK) method [33]. For the linear case, we are able to show that the proposed fully discrete scheme is *strongly stable* through the two-step and *three-step strong stability* estimates.
- (4) The theoretical convergence rates are validated through the numerical experiments. We demonstrate the rates obtained by numerical illustrations are optimal and it preserves the conserved quantity like mass and momentum in discrete set up.

The rest of the paper is organized as follows. We commence our investigation by introducing a few preliminary lemmas and semi-discrete LDG scheme in Section 2. Section 3 outlines the stability analysis and error estimate of the LDG scheme for semi-discrete. We present the stability and convergence analysis of the fully discrete Crank-Nicolson LDG scheme and prove the order of convergence  $\mathcal{O}(h^{k+1/2})$  for general nonlinear flux in Section 4. The efficiency of the scheme is validated through some numerical examples presented in Section 5. Concluding remarks and a few remarks about future work are given in Section 6.

## 2. SEMI-DISCRETE LDG SCHEME

**2.1. Preliminary results.** Hereby we describe a few relevant properties of the Hilbert transform through the following lemma. It is worthwhile to mention that these properties are instrumental for subsequent analysis.

**Lemma 2.1.** (See [24, Chapter 15]) *Let  $\phi \in L^2(\mathbb{R})$  be a sufficiently smooth function. Then the Hilbert transform  $\mathcal{H}$  satisfies the following properties:*

i) *Skew symmetric:*

$$(\mathcal{H}\phi_1, \phi_2) = -(\phi_1, \mathcal{H}\phi_2), \quad \forall \phi_1, \phi_2 \in L^2(\mathbb{R}).$$

ii) *Commutates with derivatives:*

$$\mathcal{H}\phi_x = (\mathcal{H}\phi)_x.$$

iii)  *$L^2$ -isometry property:*

$$\|\mathcal{H}\phi\|_{L^2(\mathbb{R})} = \|\phi\|_{L^2(\mathbb{R})}.$$

iv) *Orthogonality:*

$$(\mathcal{H}\phi, \phi) = 0.$$

where  $(\cdot, \cdot)$  is the standard  $L^2$ -inner product.

Given that the original problem is defined over the entire real line due to the involvement of a non-local operator  $\mathcal{H}$ , but for the numerical purpose, we restrict it to a bounded domain  $\Omega := [a, b]$ , where  $a < b$ . We assume that  $U$  has compact support within  $\Omega$ . Hence it becomes imperative to impose the boundary conditions:

$$U(a, t) = 0 = U(b, t), \quad \text{for all } t < T.$$

Moreover, the properties of the Hilbert transform introduced in Lemma 2.1 remain applicable for a bounded domain  $\Omega$ , provided  $\phi$  has a compact support within  $\Omega$ .

We partition the domain  $\Omega$  into intervals  $I_i = (x_{i-\frac{1}{2}}, x_{i+\frac{1}{2}})$  with  $a = x_{\frac{1}{2}} < x_{\frac{3}{2}} < \dots < x_{N+\frac{1}{2}} = b$ , where  $N$  represents the number of elements. This partition creates a mesh of elements denoted by  $\mathcal{I}$ , with each element having a spatial step size  $h_i = x_{i+\frac{1}{2}} - x_{i-\frac{1}{2}}$  and a maximum step size  $h = \max_{1 \leq i \leq N} \{h_i\}$ . In conjunction with this mesh, we define the broken Sobolev spaces as follows:

$$H^1(\Omega, \mathcal{I}) := \{v : \Omega \rightarrow \mathbb{R} \mid v|_{I_i} \in H^1(I_i), i = 1, \dots, N\};$$

and

$$L^2(\Omega, \mathcal{I}) := \{v : \Omega \rightarrow \mathbb{R} \mid v|_{I_i} \in L^2(I_i), i = 1, \dots, N\}.$$

Within this framework, we introduce the notation  $v_{i+\frac{1}{2}}$  to represent the value of  $v$  at the nodes  $\{x_{i+\frac{1}{2}}\}$ , and denote the one-sided limits as

$$v_{i+\frac{1}{2}}^\pm = v(x_{i+\frac{1}{2}}^\pm) := \lim_{x \rightarrow x_{i+\frac{1}{2}}^\pm} v(x).$$

We define the local inner product and local  $L^2(I_i)$  norm as follows:

$$(u, v)_{I_i} = \int_{I_i} uv \, dx, \quad \|u\|_{I_i} = (u, u)_{I_i}^{\frac{1}{2}}, \quad (u, v) = \sum_{i=1}^N (u, v)_{I_i} \quad \text{and} \quad \|u\|_{L^2(\Omega)} = \sum_{i=1}^N \|u\|_{I_i}.$$

With all these preparation we introduce the auxiliary variables  $P$  and  $Q$  such that

$$P = \mathcal{H}Q, \quad Q = U_x.$$

As a consequence, the equation (1.1) can be represented in the following equivalent form of first order differential system

$$\begin{aligned} U_t &= -(f(U) - P)_x, \\ P &= \mathcal{H}Q, \\ Q &= U_x. \end{aligned} \tag{2.1}$$

Prior to introducing the LDG scheme, we assume that the exact solution  $(U, P, Q)$  of the system (2.1) belongs to

$$\mathcal{T}_3 \times K(\Omega, \mathcal{I}) := H^1(0, T; H^1(\Omega, \mathcal{I})) \times L^2(0, T; H^1(\Omega, \mathcal{I})) \times L^2(0, T; L^2(\Omega, \mathcal{I})).$$

This implies that the solution  $(U, P, Q)$  of (2.1) satisfies the following system:

$$\begin{aligned} (U_t, v)_{I_i} &= (f(U) - P, v_x)_{I_i} - (fv - Pv) \Big|_{x_{i-\frac{1}{2}}^+}^{x_{i+\frac{1}{2}}^-}, \\ (P, w)_{I_i} &= (\mathcal{H}Q, w)_{I_i}, \\ (Q, z)_{I_i} &= -(U, z_x)_{I_i} + (Uz) \Big|_{x_{i-\frac{1}{2}}^+}^{x_{i+\frac{1}{2}}^-}, \end{aligned} \quad (2.2)$$

for all  $w \in L^2(\Omega, \mathcal{I})$ ,  $v, z \in H^1(\Omega, \mathcal{I})$ , and for  $i = 1, \dots, N$ .

We define the finite element  $V^k \subset H^1(\Omega, \mathcal{I})$  by

$$V^k = \{v \in L^2(\Omega) : v|_{I_i} \in P^k(I_i), \forall i = 1, 2, \dots, N\}, \quad (2.3)$$

where  $P^k(I_i)$  is space of polynomials of degree up to order  $k$  ( $\geq 1$ ) on  $I_i$ .

**2.2. LDG scheme.** To develop the LDG scheme for the Benjamin-Ono equation, it is necessary to define the numerical fluxes  $\hat{u}$ ,  $\hat{p}$  and the nonlinear flux  $\hat{f}$  at interfaces and boundaries. We introduce the following notations:

$$\{u\} = \frac{u^- + u^+}{2}, \quad \llbracket u \rrbracket = u^+ - u^-.$$

We choose the alternative numerical flux which is given by

$$\hat{p} = p^+, \quad \hat{u} = u^-, \quad (2.4)$$

or alternatively

$$\hat{p} = p^-, \quad \hat{u} = u^+,$$

at interface  $x_{i+\frac{1}{2}}$ ,  $i = 1, 2, \dots, N-1$ . We set the boundary flux as

$$\begin{aligned} \hat{u}_{N+\frac{1}{2}} &= U(b, t) = 0, & \hat{u}_{\frac{1}{2}} &= U(a, t) = 0, \quad \text{for all } t < T, \\ \hat{p}_{N+\frac{1}{2}} &= p_{N+\frac{1}{2}}^-, & \hat{p}_{\frac{1}{2}} &= p_{\frac{1}{2}}^+. \end{aligned} \quad (2.5)$$

For the nonlinear flux  $\hat{f}$ , we can use any monotone flux [43]. In particular, we consider the following Lax-Friedrichs flux

$$\hat{f} = \hat{f}(u^-, u^+) = \frac{1}{2}(f(u^-) + f(u^+) - \delta \llbracket u \rrbracket), \quad \delta = \max_u |f'(u)|, \quad (2.6)$$

where the maximum is taken over a range of  $u$  in a relevant element.

Applying DG approach in all the equations of the above system (2.2), we design the scheme as follows: we seek an approximations

$$(u, p, q) \in H^1(0, T; V^k) \times L^2(0, T; V^k) \times L^2(0, T; V^k) =: \mathcal{T}_3 \times \mathcal{V}^k$$

to  $(U, P, Q)$ , where  $U$  is an exact solution of (1.1) with  $P = \mathcal{H}Q$ ,  $Q = U_x$ , such that for all test functions  $(v, w, z) \in \mathcal{T}_3 \times \mathcal{V}^k$  and  $i = 1, \dots, N$ , the following system of equations holds:

$$\begin{aligned} (u_t, v)_{I_i} &= \mathcal{F}_i(f(u), v) - \mathcal{D}_i^+(p, v), \\ (p, w)_{I_i} &= (\mathcal{H}q, w)_{I_i}, \\ (q, z)_{I_i} &= -\mathcal{D}_i^-(u, z), \\ (u^0, v)_{I_i} &= (U_0, v)_{I_i}, \end{aligned} \quad (2.7)$$

where

$$\begin{aligned} \mathcal{F}_i(f(u), v) &= (f(u), v_x)_{I_i} - \hat{f}_{i+\frac{1}{2}} v_{i+\frac{1}{2}}^- + \hat{f}_{i-\frac{1}{2}} v_{i-\frac{1}{2}}^+, & \text{for } i = 1, 2, \dots, N, \\ \mathcal{D}_i^+(p, v) &= (p, v_x)_{I_i} - p_{i+\frac{1}{2}}^+ v_{i+\frac{1}{2}}^- + p_{i-\frac{1}{2}}^+ v_{i-\frac{1}{2}}^+, & \text{for } i = 1, 2, \dots, N-1, \\ \mathcal{D}_i^-(u, z) &= (u, z_x)_{I_i} - u_{i+\frac{1}{2}}^- v_{i+\frac{1}{2}}^- + u_{i-\frac{1}{2}}^- v_{i-\frac{1}{2}}^+, & \text{for } i = 1, 2, \dots, N-1, \end{aligned}$$

and

$$\mathcal{D}_N^+(p, v) = (p, v_x)_{I_N} - p_{N+\frac{1}{2}}^- v_{N+\frac{1}{2}}^- + p_{N-\frac{1}{2}}^+ v_{N-\frac{1}{2}}^+, \quad \mathcal{D}_N^-(u, z) = (u, z_x)_{I_N}.$$

The proposed LDG scheme (2.7) for the BO equation works in the following way: given  $u$ , we use the third equation of (2.7) to obtain  $q$  locally; more precisely,  $q$  in the cell  $I_i$  can be computed with the information of  $u$  in the cells  $I_{i-1}$  and  $I_i$ . Afterwards, with the help of  $q$  in the cell  $I_i$ , one can obtain  $p$  locally in the cell  $I_i$ . Finally, we update the approximate solution  $u$  in the cell  $I_i$  incorporating  $p$  and  $u$  in the cells  $I_{i-1}$  and  $I_i$ . In a similar way, for the choice of alternative fluxes  $\hat{p} = p^-$ ,  $\hat{u} = u^+$  the algorithm can be adopted accordingly.

Summing equation (2.7) over  $i = 1, 2, \dots, K$ , we have

$$\begin{aligned}(u_t, v) &= \mathcal{F}(f(u), v) + \mathcal{D}^+(p, v), \\ (p, w) &= (\mathcal{H}q, w), \\ (q, z) &= \mathcal{D}^-(u, z),\end{aligned}\tag{2.8}$$

where

$$\mathcal{F} = \sum_{i=1}^K \mathcal{F}_i \quad \text{and} \quad \mathcal{D}^\pm = - \sum_{i=1}^K \mathcal{D}_i^\pm.$$

We represent  $\mathcal{F}$ ,  $\mathcal{D}^\pm$  and associated numerical fluxes in the following way by using the simple calculations:

$$\mathcal{F}(f(u), v) = \sum_{i=1}^N (f(u), v_x)_{I_i} - \sum_{i=1}^N (\hat{f}v) \Big|_{x_{i-\frac{1}{2}}^+}^{x_{i+\frac{1}{2}}^-} = (f(u), v_x) + \hat{f}_{\frac{1}{2}} v_{\frac{1}{2}}^+ - \hat{f}_{N+\frac{1}{2}} v_{N+\frac{1}{2}}^- + \sum_{i=1}^{N-1} \hat{f}_{i+\frac{1}{2}} \llbracket v \rrbracket_{i+\frac{1}{2}},\tag{2.9}$$

$$\mathcal{D}^+(p, v) = -(p, v_x) - p_{\frac{1}{2}}^+ v_{\frac{1}{2}}^+ + p_{N+\frac{1}{2}}^- v_{N+\frac{1}{2}}^- - \sum_{i=1}^{N-1} p_{i+\frac{1}{2}}^+ \llbracket v \rrbracket_{i+\frac{1}{2}},\tag{2.10}$$

and similarly

$$\mathcal{D}^-(u, z) = -(u, z_x) - \sum_{i=1}^{N-1} u_{i+\frac{1}{2}}^- \llbracket z \rrbracket_{i+\frac{1}{2}}.\tag{2.11}$$

Moreover, we have the following result.

**Proposition 2.2.** *Let  $u$  has compact support in  $\Omega$  and  $p \in V^k$ . Then, we have*

$$\mathcal{D}^+(p, u) + \mathcal{D}^-(u, p) = 0.\tag{2.12}$$

*Proof.* Observe that, integration by parts yield the following

$$\begin{aligned}(p, u_x) + (u, p_x) &= \sum_{i=1}^N (p, u_x)_{I_i} + (u, p_x)_{I_i} = \sum_{i=1}^N (up) \Big|_{x_{i-\frac{1}{2}}^+}^{x_{i+\frac{1}{2}}^-} \\ &= -u_{\frac{1}{2}}^+ p_{\frac{1}{2}}^+ + u_{N+\frac{1}{2}}^- p_{N+\frac{1}{2}}^- - \sum_{i=1}^{N-1} u_{i+\frac{1}{2}}^- \llbracket p \rrbracket_{i+\frac{1}{2}} - \sum_{i=1}^{N-1} p_{i+\frac{1}{2}}^+ \llbracket u \rrbracket_{i+\frac{1}{2}},\end{aligned}$$

using the fact that  $u$  has compact support in  $\Omega$ , that is, (2.11) implies

$$\begin{aligned}\mathcal{D}^+(p, u) + \mathcal{D}^-(u, p) &= -(p, u_x) - (u, p_x) - p_{\frac{1}{2}}^+ u_{\frac{1}{2}}^+ + p_{N+\frac{1}{2}}^- u_{N+\frac{1}{2}}^- - \sum_{i=1}^{N-1} p_{i+\frac{1}{2}}^+ \llbracket u \rrbracket_{i+\frac{1}{2}} \\ &\quad - \sum_{i=1}^{N-1} u_{i+\frac{1}{2}}^- \llbracket p \rrbracket_{i+\frac{1}{2}} \\ &= 0.\end{aligned}$$

□

To carry out the further analysis of the LDG scheme (2.7), we define the corresponding compact form

$$\begin{aligned} \mathcal{B}(u, p, q; v, w, z) = & \sum_{i=1}^N \left[ (u_t, v)_{I_i} + (p, w)_{I_i} - (\mathcal{H}q, w)_{I_i} + (q, z)_{I_i} \right] \\ & - \mathcal{F}(f(u), v) - \mathcal{D}^+(p, v) - \mathcal{D}^-(u, z), \end{aligned} \quad (2.13)$$

for all  $(u, p, q) \in \mathcal{T}_3 \times K(\Omega, \mathcal{I})$  and  $(v, w, z) \in \mathcal{T}_3 \times \mathcal{V}^k$ .

### 3. STABILITY AND ERROR ANALYSIS

Hereby we analyze the stability and accuracy of the proposed LDG scheme (2.7) for (1.1).

**3.1. Stability of semi-discrete scheme.** We prove the following stability lemma for general flux function using an appropriate compact form:

**Lemma 3.1.** ( *$L^2$ -stability*) Let  $u, p, q$  be obtained from the LDG scheme (2.7). Then the LDG scheme (2.7) for Benjamin-Ono equation (1.1) is  $L^2$ -stable. We have the following estimate

$$\|u(\cdot, T)\|_{L^2(\Omega)} \leq C \|u^0\|_{L^2(\Omega)}, \quad (3.1)$$

for any  $T > 0$  and a constant  $C$ .

*Proof.* Since we have the compact form (2.13) of the scheme (2.7), we choose test functions  $(v, w, z) = (u, -q, p)$  in (2.13), which yields

$$\begin{aligned} \mathcal{B}(u, p, q; u, -q, p) = & \sum_{i=1}^N \left[ (u_t, u)_{I_i} - (p, q)_{I_i} + (\mathcal{H}q, q)_{I_i} + (q, p)_{I_i} \right] \\ & - \mathcal{F}(f(u), u) - \mathcal{D}^+(p, u) - \mathcal{D}^-(u, p). \end{aligned} \quad (3.2)$$

Using Proposition 2.2, estimate (2.9) and result from Lemma 2.1 in (3.2), we have

$$\mathcal{B}(u, p, q; u, -q, p) = (u_t, u) - \sum_{i=1}^N (f(u), u_x)_{I_i} - \hat{f}_{\frac{1}{2}} u_{\frac{1}{2}}^+ + \hat{f}_{N+\frac{1}{2}} u_{N+\frac{1}{2}}^- - \sum_{i=1}^{N-1} \hat{f}_{i+\frac{1}{2}} \llbracket u \rrbracket_{i+\frac{1}{2}}. \quad (3.3)$$

Let us define  $F(u) = \int^u f(u) du$ . Then we have

$$\sum_{i=1}^N (f(u), u_x)_{I_i} = \sum_{i=1}^N F(u) \Big|_{u_{i-\frac{1}{2}}^+}^{u_{i+\frac{1}{2}}^-} = - \sum_{i=1}^{N-1} \llbracket F(u) \rrbracket_{i+\frac{1}{2}} - F(u)_{\frac{1}{2}} + F(u)_{N+\frac{1}{2}}. \quad (3.4)$$

Incorporating (3.4) in equation (3.3), we have

$$\begin{aligned} \mathcal{B}(u, p, q; u, -q, p) = & (u_t, u)_{L^2(\Omega)} + \sum_{i=1}^{N-1} \llbracket F(u) \rrbracket_{i+\frac{1}{2}} + F(u)_{\frac{1}{2}} - F(u)_{N+\frac{1}{2}} \\ & - \hat{f}_{\frac{1}{2}} u_{\frac{1}{2}}^+ + \hat{f}_{N+\frac{1}{2}} u_{N+\frac{1}{2}}^- - \sum_{i=1}^{N-1} \hat{f}_{i+\frac{1}{2}} \llbracket u \rrbracket_{i+\frac{1}{2}}. \end{aligned} \quad (3.5)$$

Since  $(u, p, q)$  satisfies the LDG scheme (2.7), then we have

$$\mathcal{B}(u, p, q; v, w, z) = 0,$$

for any  $(v, w, z) \in V^k$ . As a result, we get

$$\begin{aligned} (u_t, u)_{L^2(\Omega)} + \sum_{i=1}^{N-1} \llbracket F(u) \rrbracket_{i+\frac{1}{2}} + F(u)_{\frac{1}{2}} - F(u)_{N+\frac{1}{2}} \\ - \hat{f}_{\frac{1}{2}} u_{\frac{1}{2}}^+ + \hat{f}_{N+\frac{1}{2}} u_{N+\frac{1}{2}}^- - \sum_{i=1}^{N-1} \hat{f}_{i+\frac{1}{2}} \llbracket u \rrbracket_{i+\frac{1}{2}} = 0. \end{aligned} \quad (3.6)$$

Since the numerical flux  $\hat{f} = \hat{f}(u^-, u^+)$  is monotone, it is non-decreasing in its first argument and non-increasing in its second argument. As a consequence, we have

$$\llbracket F(u) \rrbracket_{i+\frac{1}{2}} - \hat{f}_{i+\frac{1}{2}} \llbracket u \rrbracket_{i+\frac{1}{2}} > 0,$$

for all  $i = 1, 2, \dots, N-1$ . Dropping the positive term from left-hand side of equation (3.5) and using the boundary conditions, we end up with

$$\frac{1}{2} \frac{d}{dt} \|u\|_{L^2(\Omega)}^2 \leq 0. \quad (3.7)$$

Applying the Gronwall's inequality, we obtain

$$\|u(\cdot, T)\|_{L^2(\Omega)} \leq C \|u^0\|_{L^2(\Omega)}.$$

Hence the result follows.  $\square$

**3.2. Error analysis.** To advance with the error estimates, we define the projection operators into the finite element space  $V^k$  as follows. For any sufficiently smooth  $g$ , we define:

$$\begin{aligned} \int_{I_i} (\mathcal{P}^- g(x) - g(x)) y(x) dx &= 0 \quad \forall y \in P^{k-1}(I_i), \quad \text{and} \quad (\mathcal{P}^- g)_{i+1/2}^- = g(x_{i+1/2}^-), \\ \int_{I_i} (\mathcal{P} g(x) - g(x)) y(x) dx &= 0 \quad \forall y \in P^k(I_i), \end{aligned} \quad (3.8)$$

for all  $i = 1, 2, \dots, N$ . Here,  $\mathcal{P}^-$  represents a specific projection, and  $\mathcal{P}$  is the standard  $L^2$  projection. Let  $U$  be the exact solution to (1.1), and let  $u$  be the approximate solution obtained through the LDG scheme (2.7). We denote:

$$\mathcal{P}_h^- u = \mathcal{P}^- U - u, \quad \mathcal{P}_h q = \mathcal{P} Q - q,$$

and

$$\mathcal{P}_e^- U = \mathcal{P}^- U - U, \quad \mathcal{P}_e Q = \mathcal{P} Q - Q.$$

In the process of establishing the error estimate for the equation (1.1), we introduce several lemmas concerning the relationship between the physical flux  $f$  and the numerical flux  $\hat{f}$ .

**Lemma 3.2** (See Lemma 3.1 in [44]). *Let  $\xi \in L^2(\Omega)$  be any piecewise smooth function. On each interface of elements and on the boundary points we define*

$$\beta(\hat{f}; \xi) = \begin{cases} (f(\llbracket \xi \rrbracket) - \hat{f}(\xi)) \llbracket \xi \rrbracket^{-1}, & \text{if } \llbracket \xi \rrbracket \neq 0, \\ \frac{1}{2} |f'(\llbracket \xi \rrbracket)|, & \text{if } \llbracket \xi \rrbracket = 0, \end{cases}$$

where  $\hat{f}(\xi)$  is a consistent and monotone numerical flux. Then  $\beta(\hat{f}; \xi)$  is bounded and nonnegative.

Borrowing the idea from [41], we find the estimate for nonlinear part  $f(u)$ , by defining

$$\begin{aligned} \sum_{i=1}^N \mathcal{G}_i(f; U, u, v) &= \sum_{i=1}^N \int_{I_i} (f(U) - f(u)) v_x dx + \sum_{i=1}^N \left( (f(U) - f(\llbracket u \rrbracket)) \llbracket v \rrbracket \right)_{i+\frac{1}{2}} \\ &\quad + \sum_{i=1}^N \left( (f(\llbracket u \rrbracket) - \hat{f}) \llbracket v \rrbracket \right)_{i+\frac{1}{2}}. \end{aligned} \quad (3.9)$$

**Lemma 3.3** (See Corollary 3.6 in [41]). *Let the operator  $\mathcal{G}_i$ , defined by (3.9). Then we have the following estimate:*

$$\begin{aligned} \sum_{i=1}^N \mathcal{G}_i(f; U, u, v) &\leq -\frac{1}{4} \beta(\hat{f}; u) \sum_{i=1}^N \llbracket v \rrbracket_{i+\frac{1}{2}}^2 + (C + C_* h^{-1} \|U - u\|_{L^\infty(\Omega)}^2) h^{2k+1} \\ &\quad + (C + C_* (\|v\|_{L^\infty(\Omega)} + h^{-1} \|U - u\|_{L^\infty(\Omega)}^2)) \|v\|_{L^2(\Omega)}^2. \end{aligned} \quad (3.10)$$



We deal with the nonlinear flux  $f(u)$  by making an *a priori* assumption [41]. Let  $h$  be small enough and  $k \geq 1$ , then there holds

$$\|U - u\|_{L^2(\Omega)} \leq h, \quad (3.11)$$

where  $u \in V^k$  is an approximation of  $U$ . The above assumption is unnecessary for linear flux  $f(u) = u$ . We define the bilinear operator  $\mathcal{B}_0$  by the following

$$\begin{aligned} \mathcal{B}_0(u, p, q; v, w, z) &= \sum_{i=1}^N \left[ (u_t, v)_{I_i} + (p, w)_{I_i} - (\mathcal{H}q, w)_{I_i} + (q, z)_{I_i} \right] - \mathcal{D}^+(p, v) - \mathcal{D}^-(u, z) \\ &= \sum_{i=1}^N \left[ (u_t, v)_{I_i} + (p, v_x)_{I_i} + (p, w)_{I_i} - (\mathcal{H}q, w)_{I_i} + (q, z)_{I_i} + (u, z_x)_{I_i} \right] \\ &\quad + \mathcal{IF}_0(u, p; v, z), \end{aligned} \quad (3.12)$$

where the term  $\mathcal{IF}_0$  is given by

$$\mathcal{IF}_0(u, p; v, z) := p_{\frac{1}{2}}^+ v_{\frac{1}{2}}^+ - p_{N+\frac{1}{2}}^- v_{N+\frac{1}{2}}^- + \sum_{i=1}^{N-1} p_{i+\frac{1}{2}}^+ \llbracket v \rrbracket_{i+\frac{1}{2}} + \sum_{i=1}^{N-1} u_{i+\frac{1}{2}}^- \llbracket z \rrbracket_{i+\frac{1}{2}}. \quad (3.13)$$

Note that  $\mathcal{B}_0 = \mathcal{B}$  and  $\mathcal{IF}_0 = \mathcal{IF}$ , if we take  $f = 0$  in the definition of  $\mathcal{B}$  in (2.13), that is,  $\mathcal{B}_0$  is the linear part of  $\mathcal{B}$ . Incorporating (3.5) in (3.12), we have

$$\mathcal{B}_0(u, p, q; u, -q, p) = (u_t, u)_{L^2(\Omega)}. \quad (3.14)$$

**Theorem 3.4.** *Let  $U \in C^{k+1}(\Omega)$  be an exact solution of (1.1) and  $u$  be an approximate solution obtained using the LDG scheme (2.7). Then, for sufficiently small  $h$ , the following error estimate holds*

$$\|U - u\|_{L^2(\Omega)} \leq Ch^{k+1/2}, \quad (3.15)$$

where  $C$  is a constant depending on the fixed time  $T > 0$ ,  $k \geq 1$ , and the bounds on the derivatives  $|f^{(m)}|$  for  $m = 1, 2, 3$ .

*Proof.* We begin by deriving an error equation. Since  $U$  is an exact solution of (1.1), we define

$$P = Q, \quad Q = U_x.$$

Then  $U$ ,  $P$ , and  $Q$  satisfy the equation (2.13). Hence for any  $(v, w, z) \in V^k$ , we have

$$\mathcal{B}(U, P, Q; v, w, z) = \mathcal{B}(u, p, q; v, w, z) = 0,$$

where  $(u, p, q)$  is an approximate solution obtained by the scheme (2.13). By incorporating the bilinear operator  $\mathcal{B}_0$ , we get

$$\begin{aligned} 0 &= \mathcal{B}(U, P, Q; v, w, z) - \mathcal{B}(u, p, q; v, w, z) \\ &= \mathcal{B}_0(U, P, Q; v, w, z) - \mathcal{B}_0(u, p, q; v, w, z) - \sum_{i=1}^N \mathcal{G}_i(f; U, u, v) \\ &= \mathcal{B}_0(U - u, P - p, Q - q, R - r; v, w, z) - \sum_{i=1}^N \mathcal{G}_i(f; U, u, v). \end{aligned}$$

Taking into account the projection operators  $\mathcal{P}^-$  and  $\mathcal{P}$  defined in (3.8), we choose  $(v, w, z) = (\mathcal{P}_h^- u, -\mathcal{P}_h q, \mathcal{P}_h p)$ . Since  $U - u = \mathcal{Q}_h u - \mathcal{Q}_e U$ , where  $\mathcal{Q}_h = \mathcal{P}_h$  or  $\mathcal{P}_h^-$  and  $\mathcal{Q}_e = \mathcal{P}_e$  or  $\mathcal{P}_e^-$ , we have

$$\begin{aligned} \mathcal{B}_0(\mathcal{P}_h^- u, \mathcal{P}_h p, \mathcal{P}_h q; \mathcal{P}_h^- u, -\mathcal{P}_h q, \mathcal{P}_h p) &= \mathcal{B}_0(\mathcal{P}_e^- U, \mathcal{P}_e P, \mathcal{P}_e Q; \mathcal{P}_h^- u, -\mathcal{P}_h q, \mathcal{P}_h p) \\ &\quad + \sum_{i=1}^N \mathcal{G}_i(f; U, u, \mathcal{P}_h^- u). \end{aligned} \quad (3.16)$$

We estimate the first term on the right-hand side of (3.16). From equation (3.12), we have

$$\begin{aligned} \mathcal{B}_0(\mathcal{P}_e^- U, \mathcal{P}_e P, \mathcal{P}_e Q; \mathcal{P}_h^- u, -\mathcal{P}_h q, \mathcal{P}_h p) &= \sum_{i=1}^N \left[ ((\mathcal{P}_e^- U)_t, \mathcal{P}_h^- u)_{I_i} + (\mathcal{P}_e P, (\mathcal{P}_h^- u)_x)_{I_i} \right. \\ &\quad - (\mathcal{P}_e P, \mathcal{P}_h q)_{I_i} + (\mathcal{H} \mathcal{P}_e Q, \mathcal{P}_h q)_{I_i} \\ &\quad \left. + (\mathcal{P}_e Q, \mathcal{P}_h p)_{I_i} + (\mathcal{P}_e^- U, (\mathcal{P}_h p)_x)_{I_i} \right] \\ &\quad + \mathcal{IF}_0(\mathcal{P}_e^- U, \mathcal{P}_e P; \mathcal{P}_h^- u, \mathcal{P}_h p). \end{aligned} \quad (3.17)$$

Since we have

$$(\mathcal{P}_h p)_x \in P^{k-1}(I_i), \quad (\mathcal{P}_h^- u)_x \in P^{k-1}(I_i), \quad \text{and} \quad \mathcal{P}_h p, \mathcal{P}_h q \in P^k(I_i),$$

and consequently, from the projection properties defined in (3.8) and Lemma 2.1 along with the fact  $P = \mathcal{H}Q$  imply

$$\begin{aligned} (\mathcal{P}_e P, (\mathcal{P}_h^- u)_x)_{I_i} &= 0, \quad (\mathcal{P}_e Q, \mathcal{P}_h p)_{I_i} = 0, \quad (\mathcal{P}_e P - \mathcal{H} \mathcal{P}_e Q, \mathcal{P}_h q)_{I_i} = 0, \\ (\mathcal{P}_e^- U, (\mathcal{P}_h p)_x)_{I_i} &= 0, \end{aligned}$$

for all  $i = 1, 2, \dots, N$ , and  $(\mathcal{P}_e^- U)_{i+\frac{1}{2}}^- = 0$  for all  $i = 1, 2, \dots, N-1$ . Also note that, from the approximation theory on the point values associated with projection operators [9, Section 3.2], we have

$$(\mathcal{P}_e P)_{i+\frac{1}{2}}^+ \leq Ch^{k+1}, \quad (\mathcal{P}_e^- U)_{i-\frac{1}{2}}^- \leq Ch^{k+1},$$

for all  $i = 1, 2, \dots, N-1$ , and

$$(\mathcal{P}_h^- u)_{N+\frac{1}{2}}^- = 0, \quad (\mathcal{P}_h^- u)_{\frac{1}{2}}^+ = 0,$$

by using boundary conditions. Combining these error bounds and using Young's inequality, we have

$$\begin{aligned} \mathcal{IF}_0(\mathcal{P}_e^- U, \mathcal{P}_e P; \mathcal{P}_h^- u, \mathcal{P}_h p) &= (\mathcal{P}_e P)_{\frac{1}{2}}^+ (\mathcal{P}_h^- u)_{\frac{1}{2}}^+ - (\mathcal{P}_e P)_{N+\frac{1}{2}}^- (\mathcal{P}_h^- u)_{N+\frac{1}{2}}^- \\ &\quad + \sum_{i=1}^{N-1} (\mathcal{P}_e P)_{i+\frac{1}{2}}^+ \llbracket \mathcal{P}_h^- u \rrbracket_{i+\frac{1}{2}} + \sum_{i=1}^{N-1} (\mathcal{P}_e^- U)_{i+\frac{1}{2}}^- \llbracket \mathcal{P}_h p \rrbracket_{i+\frac{1}{2}} \\ &\leq \sum_{i=1}^{N-1} \left( C(\varepsilon) ((\mathcal{P}_e P)_{i+\frac{1}{2}}^+)^2 + \varepsilon \llbracket \mathcal{P}_h^- u \rrbracket_{i+\frac{1}{2}}^2 \right) \\ &\leq C(\Omega) h^{2k+1} + \varepsilon \sum_{i=1}^{N-1} \llbracket \mathcal{P}_h^- u \rrbracket_{i+\frac{1}{2}}^2, \end{aligned}$$

where  $\varepsilon > 0$ . Using the above estimates in (3.17) can be written as

$$\mathcal{B}_0(\mathcal{P}_e^- U, \mathcal{P}_e P, \mathcal{P}_e Q; \mathcal{P}_h^- u, -\mathcal{P}_h q, \mathcal{P}_h p) \leq ((\mathcal{P}_e^- U)_t, \mathcal{P}_h^- u)_{L^2(\Omega)} + C(\Omega) h^{2k+1} + \varepsilon \sum_{i=1}^{N-1} \llbracket \mathcal{P}_h^- u \rrbracket_{i+\frac{1}{2}}^2. \quad (3.18)$$

Incorporating estimates from (3.14) and (3.18) in (3.16), we have

$$\begin{aligned} ((\mathcal{P}_h^- u)_t, \mathcal{P}_h^- u)_{L^2(\Omega)} &\leq ((\mathcal{P}_e^- U)_t, \mathcal{P}_h^- u)_{L^2(\Omega)} + C(\Omega) h^{2k+1} + \varepsilon \sum_{i=1}^{N-1} \llbracket \mathcal{P}_h^- u \rrbracket_{i+\frac{1}{2}}^2 \\ &\quad + \sum_{i=1}^N \mathcal{G}_i(f; U, u, \mathcal{P}_h^- u). \end{aligned} \quad (3.19)$$

Hence estimate (3.10) and equation (3.19) imply

$$\begin{aligned}
& ((\mathcal{P}_h^- u)_t, \mathcal{P}_h^- u)_{L^2(\Omega)} + \frac{1}{4} \beta(\hat{f}; \mathcal{P}_h^- u) \sum_{i=1}^N \|\mathcal{P}_h^- u\|_{i+\frac{1}{2}}^2 \\
& \leq ((\mathcal{P}_e^- U)_t, \mathcal{P}_h^- u)_{L^2(\Omega)} + C(\Omega) h^{2k+1} + \left( C + C_* h^{-1} \|U - u\|_{L^\infty(\Omega)}^2 \right) h^{2k+1} \\
& \quad + \left( C + C_* (\|\mathcal{P}_h^- u\|_{L^\infty(\Omega)} + h^{-1} \|U - u\|_{L^\infty(\Omega)}^2) \right) \|\mathcal{P}_h^- u\|_{L^2(\Omega)}^2 + \varepsilon \sum_{i=1}^{N-1} \|\mathcal{P}_h^- u\|_{i+\frac{1}{2}}^2.
\end{aligned} \tag{3.20}$$

Utilizing the inverse property  $\|u\|_{L^\infty(\Omega)} \leq h^{-1/2} \|u\|_{L^2(\Omega)}$  and a priori assumption (3.11), we obtain the estimate

$$h^{-1} \|U - u\|_\infty^2 h^{2k+1} \leq h^{-2} \|U - u\|_{L^2(\Omega)}^2 h^{2k+1} \leq h^{2k+1}. \tag{3.21}$$

Using the above estimate and the positivity of  $\beta$  from Lemma 3.2, equation (3.20) implies

$$\frac{1}{2} \frac{d}{dt} \|\mathcal{P}_h^- u\|_{L^2(\Omega)}^2 \leq ((\mathcal{P}_e^- U)_t, \mathcal{P}_h^- u)_{L^2(\Omega)} + C(\Omega) h^{2k+1} + C \|\mathcal{P}_h^- u\|_{L^2(\Omega)}^2.$$

Using the standard approximation theory associated to the projection [9, Section 3.2], we have  $\|\mathcal{P}_h^- u(\cdot, 0)\|_{L^2(\Omega)}^2 = 0$ . Finally, with the help of Gronwall's inequality, we obtain the estimate

$$\|U - u\|_{L^2(\Omega)} \leq C h^{k+1/2}.$$

This completes the proof.  $\square$

#### 4. STABILITY AND ERROR ANALYSIS OF FULLY-DISCRETE LDG SCHEME

To develop the fully discrete local discontinuous Galerkin (LDG) scheme, we utilize the Crank-Nicolson method for time discretization in (2.8). We partition the time domain using a time step  $\tau$ . Let  $\{t^n = n\tau\}_{n=0}^M$  be the partition of the given time interval  $[0, T]$ , and define  $u^n = u(t_n)$  and  $u^{n+\frac{1}{2}} = \frac{u^{n+1} + u^n}{2}$ .

The fully discrete LDG scheme is as follows: Given  $u^n$  find  $u^{n+1}$  such that the following system holds:

$$\begin{aligned}
(u^{n+1}, v) &= (u^n, v) + \tau \mathcal{F}(f(u^{n+\frac{1}{2}}), v) + \tau \mathcal{D}^+(p^n, v), \\
(p^n, w) &= (\mathcal{H}q^n, w), \\
(q^n, z) &= \mathcal{D}^-(u^{n+\frac{1}{2}}, z),
\end{aligned} \tag{4.1}$$

for all  $v, w, z \in V^k$  and  $n = 1, 2, \dots, M-1$ , and set  $u^0 = \mathcal{P}^- u_0$ .

**Lemma 4.1.** *The fully discrete scheme (4.1) is  $L^2$ -stable, and the solution  $u^n$  obtained by the scheme (4.1) satisfies*

$$\|u^{n+1}\|_{L^2(\Omega)} \leq \|u^n\|_{L^2(\Omega)}, \quad \forall n. \tag{4.2}$$

*Proof.* We choose test functions  $(v, w, z) = (u^{n+\frac{1}{2}}, -q^n, p^n)$  in (4.1) and add all three equations to obtain

$$\left( \frac{u^{n+1} - u^n}{\tau}, u^{n+\frac{1}{2}} \right) \leq 0,$$

where we have again used the monotonicity of the numerical flux  $\hat{f}^{n+\frac{1}{2}}$ , Proposition 2.2 and Lemma 2.1. This implies

$$\|u^{n+1}\|_{L^2(\Omega)} \leq \|u^n\|_{L^2(\Omega)}, \quad \forall n.$$

This completes the proof.  $\square$

Now we aim to derive an error estimate for the fully discrete LDG scheme (4.1). We use the projection operators  $\mathcal{P}$  and  $\mathcal{P}^-$  from the previous section, defined by (3.8). Assuming that the exact solution  $U$  of (1.1) is sufficiently smooth, we want to estimate the difference  $u^n - U(t_n)$ , which is given by:

$$u^n - U(t_n) = \mathcal{P}_e^- U(t_n) - \mathcal{P}_h^- u^n, \quad (4.3)$$

where  $\mathcal{P}_e^- U(t_n) = \mathcal{P}^- U(t_n) - U(t_n)$  and  $\mathcal{P}_h^- u^n = \mathcal{P}^- U(t_n) - u^n$ . We also represent similar expressions for  $p^n - P(t_n)$  and  $q^n - Q(t_n)$ , focusing on the error estimates using projections. To carry over the semi-discrete error analysis to the fully discrete case, we need to derive an expression for the difference  $u^{n+\frac{1}{2}} - U(t_{n+\frac{1}{2}})$ , which cannot be straightforwardly expressed like the previous error term. Instead, we rewrite it as:

$$\begin{aligned} u^{n+\frac{1}{2}} - U(t_{n+\frac{1}{2}}) &= \frac{\mathcal{P}_e^- U(t_{n+1}) + \mathcal{P}_e^- U(t_n)}{2} - \frac{\mathcal{P}_h^- u^{n+1} + \mathcal{P}_h^- u^n}{2} + \rho_{n+\frac{1}{2}} \\ &=: (\mathcal{P}_e^- U)_{n+\frac{1}{2}} - (\mathcal{P}_h^- u)_{n+\frac{1}{2}} + \rho_{n+\frac{1}{2}}, \end{aligned} \quad (4.4)$$

where

$$\rho_{n+\frac{1}{2}} = \frac{U(t_{n+1}) + U(t_n)}{2} - U(t_{n+\frac{1}{2}}).$$

Using Taylor's formula with an integral remainder, we derive the following  $L^2$ -norm estimate for  $\rho_{n+\frac{1}{2}}$ :

$$\left\| \rho_{n+\frac{1}{2}} \right\|_{L^2(\Omega)}^2 \leq C\tau^3 \int_{t_n}^{t_{n+1}} \|U_{tt}(\xi)\|_{L^2(\Omega)}^2 d\xi. \quad (4.5)$$

**Theorem 4.2.** *Let  $U$  be a sufficiently smooth exact solution of the BO equation (1.1), and let  $u^n$  be the approximate solution obtained from the fully discrete LDG scheme (4.1). Then, for sufficiently small  $h$  and  $\tau$ , we have the following convergence rate*

$$\|U(t_n) - u^n\|_{L^2(\Omega)} = \mathcal{O}(h^{k+1/2} + \tau^2), \quad n = 0, 1, \dots, M, \quad (4.6)$$

provided that  $\tau \leq Ch^2$ , where constant  $C$  is independent of  $\tau$  and  $h$ .

*Proof.* We begin by expressing the scheme (4.1) in the following compact form:

$$\begin{aligned} \mathcal{B}^n(u^n, u^{n+\frac{1}{2}}, p^n, q^n; v, w, z) &= \left( \frac{u^{n+1} - u^n}{\tau}, v \right) - \mathcal{F}(f(u^{n+\frac{1}{2}}), v) - \mathcal{D}^+(p^n, v) + (p^n, w) \\ &\quad - (\mathcal{H}q^n, w) + (q^n, z) - \mathcal{D}^-(u^{n+\frac{1}{2}}, z), \end{aligned} \quad (4.7)$$

and

$$\begin{aligned} \mathcal{B}_0^n(u^n, u^{n+\frac{1}{2}}, p^n, q^n; v, w, z) &= \mathcal{B}^n(u^n, u^{n+\frac{1}{2}}, p^n, q^n; v, w, z) + \mathcal{F}(f(u^{n+\frac{1}{2}}), v) \\ &= \left( \frac{u^{n+1} - u^n}{\tau}, v \right) - \mathcal{D}^+(p^n, v) + (p^n, w) - (\mathcal{H}q^n, w) \\ &\quad + (q^n, z) - \mathcal{D}^-(u^{n+\frac{1}{2}}, z). \end{aligned} \quad (4.8)$$

Since  $u^n$  satisfies the scheme (4.1) and  $U$  is an exact solution, we have

$$\mathcal{B}^n(U(t_n), U(t_{n+\frac{1}{2}}), P(t_n), Q(t_n); v, w, z) = \mathcal{B}^n(u^n, u^{n+\frac{1}{2}}, p^n, q^n; v, w, z) = 0. \quad (4.9)$$

Therefore, using the equation (4.9), we can derive the following error equation

$$\begin{aligned} 0 &= \mathcal{B}^n(u^n, u^{n+\frac{1}{2}}, p^n, q^n; v, w, z) - \mathcal{B}^n(U(t_n), U(t_{n+\frac{1}{2}}), P(t_n), Q(t_n); v, w, z) \\ &= \mathcal{B}_0^n(u^n, u^{n+\frac{1}{2}}, p^n, q^n; v, w, z) - \mathcal{B}_0^n(U(t_n), U(t_{n+\frac{1}{2}}), P(t_n), Q(t_n); v, w, z) \\ &\quad + \sum_{i=1}^N \mathcal{G}_i(f; U(t_{n+\frac{1}{2}}), u^{n+\frac{1}{2}}, v) \\ &= \mathcal{B}_0^n(u^n - U(t_n), u^{n+\frac{1}{2}} - U(t_{n+\frac{1}{2}}), p^n - P(t_n), q^n - Q(t_n); v, w, z) \end{aligned}$$

$$\begin{aligned}
& + \sum_{i=1}^N \mathcal{G}_i(f; U(t_{n+\frac{1}{2}}), u^{n+\frac{1}{2}}, v) \\
& = \mathcal{B}_0^n(\mathcal{P}_e^- U(t_n) - \mathcal{P}_h^- u^n, (\mathcal{P}_e^- U)_{n+\frac{1}{2}} - (\mathcal{P}_h^- u)_{n+\frac{1}{2}} + \rho_{n+\frac{1}{2}}, \mathcal{P}_e P(t_n) - \mathcal{P}_h p^n, \\
& \quad \mathcal{P}_e Q(t_n) - \mathcal{P}_h q^n; v, w, z) + \sum_{i=1}^N \mathcal{G}_i(f; U(t_{n+\frac{1}{2}}), u^{n+\frac{1}{2}}, v),
\end{aligned} \tag{4.10}$$

as  $\mathcal{B}_0^n$  is a bi-linear operator. The above equation (4.10) implies the following error equation

$$\begin{aligned}
\mathcal{B}_0^n(\mathcal{P}_h^- u^n, (\mathcal{P}_h^- u)_{n+\frac{1}{2}}, \mathcal{P}_h p^n, \mathcal{P}_h q^n; v, w, z) & = \mathcal{B}_0^n(\mathcal{P}_e^- U(t_n), (\mathcal{P}_e^- U)_{n+\frac{1}{2}} + \rho_{n+\frac{1}{2}}, \mathcal{P}_e P(t_n), \\
& \quad \mathcal{P}_e Q(t_n); v, w, z) + \sum_{i=1}^N \mathcal{G}_i(f; U(t_{n+\frac{1}{2}}), u^{n+\frac{1}{2}}, v).
\end{aligned} \tag{4.11}$$

To estimate the right-hand side of equation (4.11), we choose the test function  $(v, w, z) = ((\mathcal{P}_h^- u)_{n+\frac{1}{2}}, -\mathcal{P}_h q^n, \mathcal{P}_h p^n)$ . Following the approach used in the semi-discrete error estimate, and utilizing (4.5) and (3.18) alongside the projection properties (3.8) and Young's inequality, we establish the following implications

$$\begin{aligned}
& \mathcal{B}_0^n(\mathcal{P}_e^- U(t_n), (\mathcal{P}_e^- U)_{n+\frac{1}{2}} + \rho_{n+\frac{1}{2}}, \mathcal{P}_e P(t_n), \mathcal{P}_e Q(t_n); (\mathcal{P}_h^- u)_{n+\frac{1}{2}}, -\mathcal{P}_h q^n, \mathcal{P}_h p^n) \\
& \quad + \sum_{i=1}^N \mathcal{G}_i(f; U(t_{n+\frac{1}{2}}), u^{n+\frac{1}{2}}, (\mathcal{P}_h^- u)_{n+\frac{1}{2}}) \\
& \leq \left( \frac{\mathcal{P}_e^- U(t_{n+1}) - \mathcal{P}_e^- U(t_n)}{\tau}, (\mathcal{P}_h^- u)_{n+\frac{1}{2}} \right) + C(\Omega) h^{2k+1} + \varepsilon \sum_{i=1}^{N-1} \|(\mathcal{P}_h^- u)_{n+\frac{1}{2}}\|_{i+\frac{1}{2}}^2 \\
& \quad + C(\varepsilon_1) \tau^3 \int_{t_n}^{t_{n+1}} \|U_{tt}(\xi)\|_{L^2(\Omega)}^2 d\xi + \varepsilon_1 \left\| \mathcal{H}(\mathcal{P}_h^- u)_{n+\frac{1}{2}, x} \right\|_{L^2(\Omega)}^2 \\
& \quad + \sum_{i=1}^N \mathcal{G}_i(f; U(t_{n+\frac{1}{2}}), u^{n+\frac{1}{2}}, (\mathcal{P}_h^- u)_{n+\frac{1}{2}}),
\end{aligned} \tag{4.12}$$

where  $\varepsilon, \varepsilon_1 > 0$ . Moreover, the left-hand side of (4.11) with the same test function can be expressed as follows

$$\mathcal{B}_0^n(\mathcal{P}_h^- u^n, (\mathcal{P}_h^- u)_{n+\frac{1}{2}}, \mathcal{P}_h p^n, \mathcal{P}_h q^n; (\mathcal{P}_h^- u)_{n+\frac{1}{2}}, -\mathcal{P}_h q^n, \mathcal{P}_h p^n) = \left( \frac{\mathcal{P}_h^- u^{n+1} - \mathcal{P}_h^- u^n}{\tau}, (\mathcal{P}_h^- u)_{n+\frac{1}{2}} \right). \tag{4.13}$$

Estimates (4.11), (4.12) and (4.13) along with the estimate (3.10) for nonlinear term and estimate (3.21) implies

$$\begin{aligned}
& \left( \frac{\mathcal{P}_h^- u^{n+1} - \mathcal{P}_h^- u^n}{\tau}, (\mathcal{P}_h^- u)_{n+\frac{1}{2}} \right) + \frac{1}{4} \beta(\hat{f}; (\mathcal{P}_h^- u)_{n+\frac{1}{2}}) \sum_{i=1}^N \|(\mathcal{P}_h^- u)_{n+\frac{1}{2}}\|_{i+\frac{1}{2}}^2 \\
& \leq \left( \frac{\mathcal{P}_e^- U(t_{n+1}) - \mathcal{P}_e^- U(t_n)}{\tau}, (\mathcal{P}_h^- u)_{n+\frac{1}{2}} \right) + \varepsilon \sum_{i=1}^{N-1} \|(\mathcal{P}_h^- u)_{n+\frac{1}{2}}\|_{i+\frac{1}{2}}^2 \\
& \quad + C(\varepsilon_1) \tau^3 \int_{t_n}^{t_{n+1}} \|U_{tt}(\xi)\|_{L^2(\Omega)}^2 d\xi + \varepsilon_1 \left\| \mathcal{H}(\mathcal{P}_h^- u)_{n+\frac{1}{2}, x} \right\|_{L^2(\Omega)}^2 \\
& \quad + C \left\| (\mathcal{P}_h^- u)_{n+\frac{1}{2}} \right\|_{L^2(\Omega)}^2 + C(\Omega) h^{2k+1}.
\end{aligned} \tag{4.14}$$

By applying Young's inequality, Lemma 2.1 and inverse inequality  $\left\| \mathcal{H}(\mathcal{P}_h^- u)_{n+\frac{1}{2}, x} \right\|_{L^2(\Omega)}^2 \leq \frac{1}{h^2} \left\| (\mathcal{P}_h^- u)_{n+\frac{1}{2}} \right\|_{L^2(\Omega)}^2$  in the above estimate (4.14) and also using the positivity of  $\beta$  with a suitably

small choice of  $\varepsilon$ , we obtain

$$\begin{aligned}
\frac{1}{2} \|\mathcal{P}_h^- u^{n+1}\|_{L^2(\Omega)}^2 &\leq \frac{1}{2} \|\mathcal{P}_h^- u^n\|_{L^2(\Omega)}^2 + C(\varepsilon_2) \|\mathcal{P}_e^- U(t_{n+1})\|_{L^2(\Omega)}^2 + C(\varepsilon_2) \|\mathcal{P}_e^- U(t_n)\|_{L^2(\Omega)}^2 \\
&\quad + \varepsilon_2 \tau \|\mathcal{P}_h^- u^{n+1}\|_{L^2(\Omega)}^2 + \varepsilon_2 \tau \|\mathcal{P}_h^- u^n\|_{L^2(\Omega)}^2 \\
&\quad + C(\varepsilon_1) \tau^4 \int_{t_n}^{t_{n+1}} \|U_{tt}(\xi)\|_{L^2(\Omega)}^2 d\xi + \frac{\tau}{h^2} \varepsilon_1 \left\| (\mathcal{P}_h^- u)_{n+\frac{1}{2}} \right\|_{L^2(\Omega)}^2 \\
&\quad + C\tau \left\| (\mathcal{P}_h^- u)_{n+\frac{1}{2}} \right\|_{L^2(\Omega)}^2 + C(\Omega) \tau h^{2k+1}.
\end{aligned} \tag{4.15}$$

We now employ the CFL condition  $\frac{\tau}{h^2} \leq C$ , along with the choice of a small  $\varepsilon_1$  and the triangle inequality in (4.15), which yields

$$\begin{aligned}
\|\mathcal{P}_h^- u^{n+1}\|_{L^2(\Omega)}^2 &\leq \frac{1+C\tau}{1-C\tau} \|\mathcal{P}_h^- u^n\|_{L^2(\Omega)}^2 + C(\varepsilon_1) \tau^4 \int_{t_n}^{t_{n+1}} \|U_{tt}(\xi)\|_{L^2(\Omega)}^2 d\xi + C(\Omega) \tau h^{2k+1} \\
&\leq \left( \frac{1+C\tau}{1-C\tau} \right)^n \|\mathcal{P}_h^- u^0\|_{L^2(\Omega)}^2 + C(\varepsilon_1) \tau^4 \sum_{k=0}^{n-1} \left( \frac{1+C\tau}{1-C\tau} \right)^{n-k} \int_{t_k}^{t_{k+1}} \|U_{tt}(\xi)\|_{L^2(\Omega)}^2 d\xi \\
&\quad + C(\Omega) n \tau h^{2k+1} \\
&\leq e^{4CT} \|\mathcal{P}_h^- u^0\|_{L^2(\Omega)}^2 + e^{4CT} \tau^4 \int_0^T \|U_{tt}(\xi)\|_{L^2(\Omega)}^2 d\xi + C(\Omega) T h^{2k+1}.
\end{aligned} \tag{4.16}$$

Since  $U$  is smooth and  $\mathcal{P}_h^- u^0 = 0$ , the following estimate holds

$$\|\mathcal{P}_h^- u^{n+1}\|_{L^2(\Omega)} \leq C(u^0, T)(h^{k+1/2} + \tau^2).$$

This completes the proof.  $\square$

**4.1. Stability analysis of higher order LDG scheme for linearized Benjamin-Ono equation.** Hereby we focus on the stability analysis with an explicit fourth-order Runge-Kutta time discretization. The spatial stability of LDG schemes are demonstrated in Section 3. It is worth mentioning that the stability analysis under the higher-order time discretizations is a challenging task, and at present we have pursued this analysis exclusively in the linear case. In particular, for simplicity, we choose the flux function  $f(U) = 0$ .

Then the semi-discrete scheme (2.7) corresponds to an ODE system

$$\frac{d}{dt} u = L_h u. \tag{4.17}$$

where LDG operator  $L_h$  can be recovered from the semi-discrete scheme (2.7). We consider the four-stage explicit fourth-order RK method for time discretization [33]:

$$u^{n+1} = P_4(\Delta t L_h) u^n, \tag{4.18}$$

where the operator  $P_4$  is given by

$$P_4(\Delta t L_h) = I + \Delta t L_h + \frac{1}{2}(\Delta t L_h)^2 + \frac{1}{6}(\Delta t L_h)^3 + \frac{1}{24}(\Delta t L_h)^4.$$

We introduce some notations which will be used frequently in subsequent stability analysis.

- We say that the LDG operator  $L_h$  is semi-negative if  $(v, (L_h + L_h^T)v) \leq 0$ ,  $\forall v \in V^k$ . Moreover, we denote it by  $L_h + L_h^T \leq 0$ .
- We define  $[u, v] = -(u, (L_h + L_h^T)v)$ . It is a bilinear form on  $V^k$ .
- We denote  $\mathcal{L}_h := \Delta t L_h$ .

We introduce few definitions which are instrumental for the stability analysis.

**Definition 4.3** (Strong stability). *Let  $u^n$  be the approximate solution obtained by the fully discrete scheme (4.18). Then the scheme (4.18) is said to be strongly stable if there exists an integer  $n_0$ , such that*

$$\|u^n\|_{L^2(\Omega)} \leq \|u^0\|_{L^2(\Omega)}, \quad \forall n \geq n_0, \quad (4.19)$$

*provided CFL number is sufficiently small.*

**Definition 4.4** (Monotonicity stability). *Let  $u^n$  be the approximate solution obtained by the fully discrete scheme (4.18). Then the scheme (4.18) is said to have monotonicity stability, if we have*

$$\|u^{n+1}\|_{L^2(\Omega)} \leq \|u^n\|_{L^2(\Omega)}, \quad \forall n \geq 0, \quad (4.20)$$

*provided CFL number is sufficiently small. Moreover, monotonicity stability implies the strong stability.*

**Lemma 4.5** (Energy equality [33]). *Let  $u^n$  be the solution of fully discrete scheme (4.18). Then*

$$\|u^{n+1}\|_{L^2(\Omega)}^2 - \|u^n\|_{L^2(\Omega)}^2 = \mathcal{Q}(u^n), \quad \forall n \geq 1,$$

*where*

$$\mathcal{Q}(u^n) = \frac{1}{576} \|\mathcal{L}_h^4 u^n\|_{L^2(\Omega)}^2 - \frac{1}{72} \|\mathcal{L}_h^3 u^n\|_{L^2(\Omega)}^2 + \Delta t \sum_{i,j=0}^3 \alpha_{ij} [\mathcal{L}_h^i u^n, \mathcal{L}_h^j u^n],$$

*and*

$$A = (\alpha_{ij})_{i,j=0}^3 = - \begin{pmatrix} 1 & 1/2 & 1/6 & 1/24 \\ 1/2 & 1/3 & 1/8 & 1/24 \\ 1/6 & 1/8 & 1/24 & 1/48 \\ 1/24 & 1/24 & 1/48 & 1/144 \end{pmatrix}.$$

In Lemma 4.5,  $\mathcal{Q}(u^n)$  is referred as the energy change of the approximate solution, consisting of two components: the numerical dissipation  $\frac{1}{576} \|\mathcal{L}_h^4 u^n\|_{L^2(\Omega)}^2 - \frac{1}{72} \|\mathcal{L}_h^3 u^n\|_{L^2(\Omega)}^2$  and the quadratic form  $\Delta t \sum_{i,j=0}^3 \alpha_{ij} [\mathcal{L}_h^i u^n, \mathcal{L}_h^j u^n]$ . The next lemma establishes the negativity of the quadratic form, also provides conditions for the strong stability.

**Lemma 4.6** (See Lemma 2.4 in [33]). *Let  $L_h$  be a semi-negative operator and*

$$\mathcal{Q}_1(u) = \zeta \|\mathcal{L}_h^3(u)\|_{L^2(\Omega)} + \Delta t \sum_{i,j=0}^m \bar{\alpha}_{ij} [\mathcal{L}_h^i u, \mathcal{L}_h^j u], \quad (4.21)$$

*where  $\bar{\alpha}_{ij} = \bar{\alpha}_{ji}$  and  $m \geq 2$ . If  $\zeta < 0$  and  $\bar{A} = (\bar{\alpha}_{ij})_{i,j=0}^m$  is negative definite, then there exists a constant  $c_0 > 0$  such that  $\mathcal{Q}_1(u) \leq 0$  provided  $\|L_h\| \leq c_0$ .*

For simplicity, we are using uniform time stepping. Since the semi-discrete scheme (2.7) is spatially stable from the Lemma 3.1, that is

$$\left( \frac{d}{dt} u, u \right) = (L_h u, u) \leq 0,$$

the LDG operator  $L_h$  is semi-negative [32] by the following

$$\left( \frac{d}{dt} u, u \right) = (L_h u, u) = \frac{1}{2} (L_h u, u) + \frac{1}{2} (u, L_h u) = \frac{1}{2} ((L_h + L_h^T) u, u) \leq 0,$$

implies  $L_h + L_h^T \leq 0$ .

The question of whether the classical fourth-order Runge-Kutta method is strongly stable or not remained open until Sun and Shu partially addressed it in [33], where they provided a counterexample showing that this method is not always strongly stable for semi-negative operators. However, it is worth noting that the semi-negative operator provided in the counterexample in [33] is not a DG operator. Another counterexample is presented in [39, Section 6], illustrating that this method does not have monotonicity stability for semi-negative DG operators. However, in [33], it was demonstrated that applying the classical fourth-order Runge-Kutta scheme for two

consecutive time steps, which can be viewed as an eight-stage, fourth-order Runge-Kutta method, is strongly stable for semi-negative operators.

**Theorem 4.7** (Two-step strong stability [33]). *Let  $L_h + L_h^T \leq 0$ . Then the four-stage fourth-order RK scheme (4.18) is strongly stable in two steps and we have*

$$\|u^{n+2}\|_{L^2(\Omega)} \leq \|u^n\|_{L^2(\Omega)},$$

provided  $\Delta t \|L_h\| \leq c_0$ , where  $c_0$  is a constant and  $\|\cdot\|$  is an operator norm.

Recently, Sun and Shu in [32] have further generalize their results obtained in [33] for showing stability of fully discrete Runge-Kutta scheme for semi-negative operators. We follow the idea from [33] to prove that the scheme is strongly stable in three steps in the following theorem which helps us to show the scheme (4.18) is strongly stable in the sense of Definition 4.19.

**Theorem 4.8** (Three-step strong stability). *Let  $L_h + L_h^T \leq 0$ . Then the four-stage fourth-order RK scheme (4.18) is strongly stable in three steps. Therefore, we have*

$$\|u^{n+3}\|_{L^2(\Omega)} \leq \|u^n\|_{L^2(\Omega)}, \quad n \geq 0,$$

provided  $\Delta t \|L_h\| \leq c_0$ , where  $c_0$  is a constant.

*Proof.* From the Lemma 4.5, energy equality implies

$$\|u^{n+3}\|_{L^2(\Omega)}^2 - \|u^n\|_{L^2(\Omega)}^2 = \mathcal{Q}(u^{n+2}) + \mathcal{Q}(u^{n+1}) + \mathcal{Q}(u^n), \quad (4.22)$$

where  $\mathcal{Q}(u^n)$  is defined in Lemma 4.5. We find the estimates for  $\mathcal{Q}(u^{n+1})$  and  $\mathcal{Q}(u^{n+2})$  in terms of  $u^n$  in its quadratic part by the following calculation:

$$\begin{aligned} \mathcal{Q}(u^{n+1}) &= \frac{1}{576} \|\mathcal{L}_h^4 u^{n+1}\|_{L^2(\Omega)}^2 - \frac{1}{72} \|\mathcal{L}_h^3 u^{n+1}\|_{L^2(\Omega)}^2 + \Delta t \sum_{i,j=0}^3 \alpha_{ij} [\mathcal{L}_h^i u^{n+1}, \mathcal{L}_h^j u^{n+1}] \\ &= \frac{1}{576} \|\mathcal{L}_h^4 u^{n+1}\|_{L^2(\Omega)}^2 - \frac{1}{72} \|\mathcal{L}_h^3 u^{n+1}\|_{L^2(\Omega)}^2 + \Delta t \sum_{i,j=0}^3 \alpha_{ij} [\mathcal{L}_h^i P_4(\mathcal{L}_h) u^n, \mathcal{L}_h^j P_4(\mathcal{L}_h) u^n] \\ &= \frac{1}{576} \|\mathcal{L}_h^4 u^{n+1}\|_{L^2(\Omega)}^2 - \frac{1}{72} \|\mathcal{L}_h^3 u^{n+1}\|_{L^2(\Omega)}^2 + \Delta t \sum_{i,j=0}^7 \tilde{\alpha}_{ij} [\mathcal{L}_h^i u^n, \mathcal{L}_h^j u^n], \end{aligned}$$

where

$$A_0 = (\alpha_{ij})_{i,j=0}^2 = - \begin{pmatrix} 1 & 1/2 & 1/6 \\ 1/2 & 1/3 & 1/8 \\ 1/6 & 1/8 & 1/24 \end{pmatrix}, \quad A_1 = (\tilde{\alpha}_{ij})_{i,j=0}^2 = - \begin{pmatrix} 1 & 3/2 & 7/6 \\ 3/2 & 7/3 & 15/8 \\ 7/6 & 15/8 & 37/24 \end{pmatrix},$$

as our interest in the first  $3 \times 3$  coefficient matrix, it is important to note that this is sufficient to apply the result in Lemma 4.6. While the complete matrix can be obtained and is not difficult, it involves a lengthy derivation. For brevity, we choose not to provide the complete matrix here, and we refer to [33] for detailed information.

In a similar way, we obtain

$$\begin{aligned} \mathcal{Q}(u^{n+2}) &= \frac{1}{576} \|\mathcal{L}_h^4 u^{n+2}\|_{L^2(\Omega)}^2 - \frac{1}{72} \|\mathcal{L}_h^3 u^{n+2}\|_{L^2(\Omega)}^2 + \Delta t \sum_{i,j=0}^3 \alpha_{ij} [\mathcal{L}_h^i u^{n+2}, \mathcal{L}_h^j u^{n+2}] \\ &= \frac{1}{576} \|\mathcal{L}_h^4 u^{n+2}\|_{L^2(\Omega)}^2 - \frac{1}{72} \|\mathcal{L}_h^3 u^{n+2}\|_{L^2(\Omega)}^2 + \Delta t \sum_{i,j=0}^7 \tilde{\alpha}_{ij} [\mathcal{L}_h^i u^{n+1}, \mathcal{L}_h^j u^{n+1}] \\ &= \frac{1}{576} \|\mathcal{L}_h^4 u^{n+2}\|_{L^2(\Omega)}^2 - \frac{1}{72} \|\mathcal{L}_h^3 u^{n+2}\|_{L^2(\Omega)}^2 + \Delta t \sum_{i,j=0}^7 \tilde{\alpha}_{ij} [\mathcal{L}_h^i P_4(\mathcal{L}_h) u^n, \mathcal{L}_h^j P_4(\mathcal{L}_h) u^n] \\ &= \frac{1}{576} \|\mathcal{L}_h^4 u^{n+2}\|_{L^2(\Omega)}^2 - \frac{1}{72} \|\mathcal{L}_h^3 u^{n+2}\|_{L^2(\Omega)}^2 + \Delta t \sum_{i,j=0}^{11} \hat{\alpha}_{ij} [\mathcal{L}_h^i u^n, \mathcal{L}_h^j u^n], \end{aligned}$$



where

$$A_2 = (\hat{\alpha}_{ij})_{i,j=0}^2 = - \begin{pmatrix} 1 & 5/2 & 19/6 \\ 5/2 & 19/3 & 57/8 \\ 19/6 & 57/8 & 253/24 \end{pmatrix}.$$

Assuming  $\|\mathcal{L}_h\| \leq 2$ , we have the following estimates

$$\begin{aligned} \frac{1}{576} \|\mathcal{L}_h^4 u^{n+2}\|_{L^2(\Omega)}^2 - \frac{1}{72} \|\mathcal{L}_h^3 u^{n+2}\|_{L^2(\Omega)}^2 &\leq 0, \\ \frac{1}{576} \|\mathcal{L}_h^4 u^{n+1}\|_{L^2(\Omega)}^2 - \frac{1}{72} \|\mathcal{L}_h^3 u^{n+1}\|_{L^2(\Omega)}^2 &\leq 0, \\ \frac{1}{576} \|\mathcal{L}_h^4 u^n\|_{L^2(\Omega)}^2 - \frac{1}{72} \|\mathcal{L}_h^3 u^n\|_{L^2(\Omega)}^2 &\leq -\frac{1}{144} \|\mathcal{L}_h^3 u^n\|_{L^2(\Omega)}^2. \end{aligned}$$

Hence (4.22) becomes

$$\|u^{n+3}\|_{L^2(\Omega)}^2 - \|u^n\|_{L^2(\Omega)}^2 \leq -\frac{1}{144} \|\mathcal{L}_h^3 u^n\|_{L^2(\Omega)}^2 + \Delta t \sum_{i,j=0}^{11} \bar{\alpha}_{ij} [\mathcal{L}_h^i u^n, \mathcal{L}_h^j u^n] =: \mathcal{Q}_1(u^n),$$

where

$$A = (\bar{\alpha}_{ij})_{i,j=0}^2 = (\alpha_{ij})_{i,j=0}^2 + (\tilde{\alpha}_{ij})_{i,j=0}^2 + (\hat{\alpha}_{ij})_{i,j=0}^2 = - \begin{pmatrix} 3 & 9/2 & 9/2 \\ 9/2 & 9 & 73/8 \\ 9/2 & 73/8 & 97/8 \end{pmatrix}.$$

Since the eigenvalues of  $A$  are -21.9444, -1.64399 and -0.536623, it follows that  $A$  is negative definite. Applying the Lemma 4.6, we obtain  $\mathcal{Q}_1(u^n) \leq 0$ . Hence

$$\|u^{n+3}\|_{L^2(\Omega)} \leq \|u^n\|_{L^2(\Omega)}.$$

This completes the proof.  $\square$

Stability in two and three steps of the fully discrete LDG scheme (4.18) combined together proves the following theorem.

**Theorem 4.9.** *Let  $L_h + L_h^T \leq 0$ . Then the four-stage fourth-order RK LDG scheme (4.18) is strongly stable. That is, we have*

$$\|u^n\|_{L^2(\Omega)} \leq \|u^0\|_{L^2(\Omega)}, \quad \forall n \geq 2,$$

provided  $\Delta t \|L_h\| \leq c_0$ , where  $c_0$  is a constant.

## 5. NUMERICAL EXPERIMENTS

In this section, our goal is to validate the proposed LDG scheme (2.7) for the Benjamin-Ono (BO) equation (1.1). We begin our numerical validation using the Crank-Nicolson (CN) LDG scheme (4.1) with  $\tau = 0.5h^2$  and  $k = 1$ . To compute the Hilbert transform of the approximation  $q$  of  $Q = U_x$  in the scheme (2.7), we utilize the fast Fourier transform. Consequently, we employ the periodic solution of the Benjamin-Ono equation. It is important to note that since the implicit term appears in the nonlinear part of the scheme (4.1), we use Newton iteration to solve it at each time step.

Order of convergence for errors is defined for each intermediate step between element numbers  $N_1$  and  $N_2$  as

$$\text{order} = \frac{\ln(E(N_1)) - \ln(E(N_2))}{\ln(N_2) - \ln(N_1)},$$

where  $L^2$  error  $E$  can be seen as a function of number of elements  $N$ . The BO equation (1.1) possesses an infinite number of conserved quantities [16]. Hereby we consider the first two specific quantities known as *mass* and *momentum* and with normalization, these quantities can be expressed as follows:

$$\mathbf{C}_1 := \frac{\int_{\Omega} u \, dx}{\int_{\Omega} U_0 \, dx}, \quad \mathbf{C}_2 := \frac{\|u\|_{L^2(\Omega)}}{\|U_0\|_{L^2(\Omega)}}.$$

Our aim is to preserve these quantities in the discrete set up.

We compare approximate solution  $u$  obtained by (4.1) with the exact periodic solution of the Benjamin-Ono equation (1.1) with  $f(U) = \frac{1}{2}U^2$ . For instance, we consider the solution of (1.1) from Thomée et. al. [35] (also see [13, 14])

$$U(x, t) = \frac{2c\delta}{1 - \sqrt{1 - \delta^2} \cos(c\delta(x - ct))}, \quad \delta = \frac{\pi}{cL}, \quad (5.1)$$

where we choose  $L = 15$ ,  $c = 0.25$ . We compare the above exact solution at the final time  $T = 20$ . This solution characterizes periodic solitary waves, exhibiting periodicity and amplitude determined by the parameters  $L$  and  $c$  respectively. Table 5.2 presents the  $L^2$ -errors of the proposed fully discrete CN-LDG scheme (4.1) using a polynomial of degree one. The results confirm that the numerically obtained rates are optimal and that the approximate solution  $u$  converges to the exact solution  $U$ .

N	error	order	C <sub>1</sub>	C <sub>2</sub>
160	1.65e-02	2.14	1.04	0.97
320	3.77e-03		1.05	0.97
640	8.98e-04	2.07	1.02	0.98
1280	2.18e-04	2.04	1.00	1.00

TABLE 5.1.  $L^2$ -error and order of convergence for the CN-LDG scheme at time  $T = 20$  taking  $N$  elements and polynomial degree  $k = 1$ .

To achieve the better accuracy in time, we perform the numerical results using the four stage fourth order explicit Runge-Kutta scheme (4.18). Our focus lies on verifying the performance of the scheme using a low storage explicit Runge-Kutta (LSERK) of fourth order time discretization [7, 15, 18] of the form

$$\begin{aligned} r^{(0)} &= u_h^n, \\ \text{for } j &= 1 : 5 \\ &\begin{cases} k^j = a_j k^{j-1} + \Delta t L_h r^{(j-1)}, \\ r^{(j)} = r^{(j-1)} + b_j k^j, \end{cases} \\ u_h^{n+1} &= r^{(5)}, \end{aligned}$$

where the weighted coefficients  $a_j$ ,  $b_j$  and  $c_j$  of the LSERK method given in [18]. The above defined iteration is equivalent to the classical fourth order method (4.18) [18]. LSERK is considerably more efficient and accurate than (4.18) since it has the disadvantage that it requires four extra storage arrays. We are providing the steps of algorithm to compute the approximate solution using LDG scheme (2.7) with LSERK time discretization, for more details one may refer to [18].

In numerical implementation with LSERK time discretization, we initially compare the approximate solution obtained from the LDG scheme (2.7) with the exact solution (5.1) at time  $t = 10$ , and further at the final time  $t = 20$ . Figure 5.1 depicts the comparison of the solution at various times. This validation confirms that the numerical scheme converges to the exact solution. The Table 5.2 presents the  $L^2$ -errors of the proposed scheme under polynomial degree up to three. It is observed that the errors are converging to zero with relatively coarser grids and optimal orders of convergence are obtained at time  $T = 10$  for each polynomial degree up to three and the discrete conserved quantities  $C_1$  and  $C_2$  are also preserved. Similar analysis has been carried out at time  $T = 20$  and details are presented in Table 5.3 and optimal rates are obtained there as well.

We have also approached to compute the Hilbert transform of the approximation by using Gaussian quadrature. However, we do not achieve the optimal rates or the theoretical rates obtained by convergence analysis. Similar observations are also described in [16, Section 5]. One possible interpretation is that the principal value integral is not being computed accurately near the

**Algorithm 1** Numerical Procedure for Benjamin-Ono Equation

---

```

1: Set up problem parameters and initial conditions
2: Compute time step size  $dt$  based on CFL condition
3: Determine total number of time steps  $Nsteps$  based on Final time and  $dt$ 
4: for  $tstep = 1$  to  $Nsteps$  do
5:   for  $INTRK = 1$  to  $5$  do
6:     Compute local time  $timelocal$  for current stage
7:     Evaluate right-hand side  $Lu$  of the differential equation using Algorithm 2
8:     Update solution  $u$  using Runge-Kutta stages
9:   end for
10:  Increment time by  $dt$ 
11: end for
12: return Final solution  $u$ 

```

---

**Algorithm 2** Algorithm for Computing RHS of Benjamin-Ono Equation**Require:** Solution  $u$ , left boundary value  $xL$ , right boundary value  $xR$ , current time  $timelocal$ **Ensure:** Right-hand side of the equation  $rhsu$ 

```

1: Compute coefficients and variables based on initial conditions and boundary values
2: Define field differences at interfaces, including boundary conditions
3: Compute flux for  $u$ 
4: Compute local variable  $q$  and its differences using  $u$ 
5: Compute local variable  $p$ , using Hilbert transform of  $q$ 
6: Compute flux for  $p$  ( $fluxp$ )
7: Compute squared differences of  $u$ ,  $du^2$  at interfaces, and impose boundary conditions
8: Compute flux for the convective term ( $fluxf$ )
9: Compute derivative of the flux ( $dfdr$ )
10: Compute right-hand side of the semi-discrete PDE ( $rhsu$ )
11: return  $rhsu$ 

```

---

singularity, and it is most likely caused by our approximation of the full line problem by restricting to a bounded interval while still employing the full line Hilbert transform.

k	k=1		k=2		k=3			
N	error	order	error	order	error	order	C <sub>1</sub>	C <sub>2</sub>
40	2.91e-01	2.01	3.65e-02	2.76	8.69e-03	4.37	1.01	1.01
80	7.15e-02		5.37e-03	2.93	4.20e-04	4.07	1.00	1.00
160	1.77e-02		7.029e-04	2.98	2.49e-05	4.00	1.00	1.00
320	4.40e-03		8.88e-05		1.56e-06		1.00	1.00

TABLE 5.2.  $L^2$ -error and order of convergence for the RK-LDG scheme at time  $T = 10$  taking  $N$  elements and polynomial degree  $k$  with normalized conserved quantities  $C_1$  and  $C_2$ .

## 6. CONCLUDING REMARKS

We have designed a local discontinuous Galerkin method for the Benjamin-Ono equation with general nonlinear flux. We have shown that the semi-discrete scheme is stable and convergent. The stability and convergence analysis is also carried out for fully discrete Crank-Nicolson LDG scheme considering any general nonlinear flux function. The convergence analysis for fully-discrete scheme

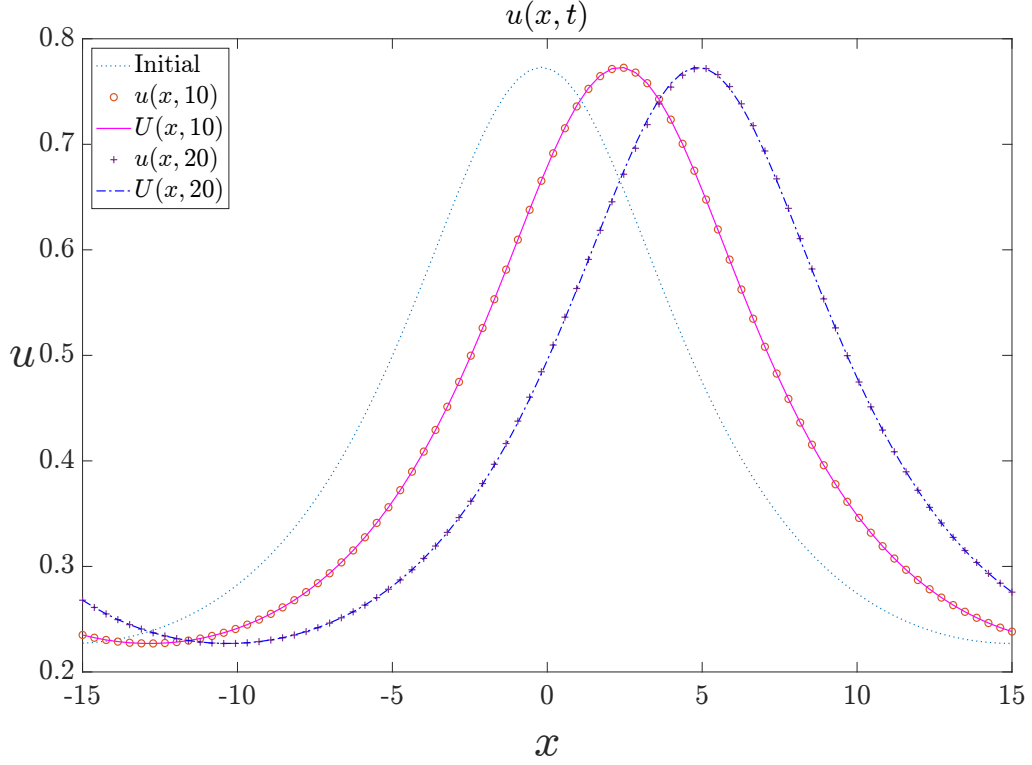


FIGURE 5.1. Exact  $U(x, t)$  and approximate solution  $u(x, t)$  computed by the RK-LDG scheme at  $T = 10$  and  $T = 20$  with  $N = 160$ ,  $k = 3$  and initial condition  $U(x, 0)$  of (1.1).

<b>k</b>	<b>k=1</b>		<b>k=2</b>		<b>k=3</b>			
<b>N</b>	<b>error</b>	<b>order</b>	<b>error</b>	<b>order</b>	<b>error</b>	<b>order</b>	<b>C<sub>1</sub></b>	<b>C<sub>2</sub></b>
<b>40</b>	6.02e-01	2.05	6.015e-01	2.65	5.98e-02	4.46	0.99	0.98
<b>80</b>	1.45e-01		9.54e-02	2.90	2.718e-03	4.09	1.00	1.00
<b>160</b>	3.56e-02	2.01	1.27e-02	2.97	1.59e-04	4.02	1.00	1.00
<b>320</b>	8.83e-03		1.62e-03		9.80e-06		1.00	1.00

TABLE 5.3.  $L^2$ -error and order of convergence for the RK-LDG scheme at time  $T = 20$  taking  $N$  elements and polynomial degree  $k$  with normalized conserved quantities  $C_1$  and  $C_2$ .

incorporating fourth order Runge-Kutta time marching scheme will be addressed in the future work. In the numerical experiments, it is observed that optimal rates are obtained for various degrees of polynomials which demonstrates the efficiency and accuracy of the proposed scheme.

#### REFERENCES

- [1] M. J. Ablowitz and A. S. Fokas. The inverse scattering transform for the Benjamin-Ono equation—a pivot to multidimensional problems. *Studies in Applied Mathematics*, 68 (1983), no. 1, 1-10.
- [2] T. Aboelenen. A high-order nodal discontinuous Galerkin method for nonlinear fractional Schrödinger type equations. *Communications in Nonlinear Science and Numerical Simulation*, 54 (2018), 428-452.

- [3] J. Ai, Y. Xu, C.-W. Shu and Q. Zhang.  $L^2$  error estimate to smooth solutions of high order Runge-Kutta discontinuous Galerkin method for scalar nonlinear conservation laws with and without sonic points. *SIAM Journal on Numerical Analysis*, 60 (2022), no. 4, 1741-1773.
- [4] F. Bassi and S. Rebay. A high-order accurate discontinuous finite element method for the numerical solution of the compressible Navier-Stokes equations. *Journal of Computational Physics*, 131 (1997), no. 2, 267-279.
- [5] N. Burq and F. Planchon. On well-posedness for the Benjamin-Ono equation. *Mathematische Annalen*, 340 (2008), no. 3, 497-542.
- [6] M.P. Calvo, J. De Frutos and J. Novo. Linearly implicit Runge-Kutta methods for advection-reaction-diffusion equations. *Applied Numerical Mathematics*, 37 (2001), no. 4, 535-549.
- [7] H. M. Carpenter and A. C. Kennedy. Fourth-order 2N-storage Runge-Kutta schemes. *NASA TM 109112*, NASA Langley Research Center, 1994.
- [8] K. M. Case. Benjamin-Ono related equations and their solutions. *Proceedings of the National Academy of Sciences*, 76 (1979), no. 1, 1-3.
- [9] P. G. Ciarlet. The finite element method for elliptic problems. *Society for Industrial and Applied Mathematics*, 2002.
- [10] B. Cockburn, G. E. Karniadakis and C.-W. Shu. Discontinuous Galerkin methods: theory, computation and applications. *Springer Science & Business Media*, 2012.
- [11] B. Cockburn and C.-W. Shu. The local discontinuous Galerkin method for time-dependent convection-diffusion systems. *SIAM Journal on Numerical Analysis*, 35 (1998), no. 6, 2440-2463.
- [12] R. Dutta, H. Holden, U. Koley and N. H. Risebro. Convergence of finite difference schemes for the Benjamin-Ono equation. *Numerische Mathematik*, 134 (2016), no. 2, 249-274.
- [13] M. Dwivedi and T. Sarkar. Stability and convergence analysis of a Crank-Nicolson Galerkin scheme for the fractional Korteweg-de Vries equation. *The SMAI Journal of computational mathematics*, 10 (2024), 107-139.
- [14] M. Dwivedi and T. Sarkar. Fully discrete finite difference schemes for the fractional Korteweg-de Vries equation. *arXiv preprint [arXiv:2403.08275](https://arxiv.org/abs/2403.08275)*, (2024).
- [15] M. Dwivedi and T. Sarkar. Local discontinuous Galerkin method for fractional Korteweg-de Vries equation. *arXiv preprint [arXiv:2404.18069](https://arxiv.org/abs/2404.18069)*, (2024).
- [16] S. T. Galtung. Convergent Crank-Nicolson Galerkin scheme for the Benjamin-Ono equation. *Discrete and Continuous Dynamical Systems*, 38 (2018), no. 3, 1243-1268.
- [17] S. T. Galtung. Convergence rates of a fully discrete Galerkin scheme for the Benjamin-Ono equation. *XVI International Conference on Hyperbolic Problems: Theory, Numerics, Applications*, Springer, (2016), 589-601.
- [18] J. S. Hesthaven and T. Warburton. Nodal discontinuous Galerkin methods: algorithms, analysis, and applications. *Springer Science and Business Media*, 2007.
- [19] J. Hunter, Z. Sun and Y. Xing. Stability and time-step constraints of implicit-explicit Runge-Kutta methods for the linearized Korteweg-de Vries equation. *Communications on Applied Mathematics and Computation*, (2023), 1-30.
- [20] A. Ionescu and C. E. Kenig. Global well-posedness of the Benjamin-Ono equation in low-regularity spaces. *Journal of the American Mathematical Society*, 20 (2007), no. 3, 753-798.
- [21] R. J. Iório. On the Cauchy problem for the Benjamin-Ono equation. *Communications in Partial Differential Equations*, 11 (1986), no. 10, 1031-1081.
- [22] Y. Ishimori. Solitons in a one-dimensional Lennard-Jones lattice. *Progress of Theoretical Physics*, 68 (1982), no. 2, 402-410.
- [23] C. E. Kenig and K. D. Koenig. On the local well-posedness of the Benjamin-Ono and modified Benjamin-Ono equations. *Mathematical Research Letters*, 10 (2003), no. 6, 879-895.
- [24] F. W. King. Hilbert transforms: Volume 2. *Cambridge University Press*, 2009.
- [25] H. Koch and N. Tzvetkov. On the local well-posedness of the Benjamin-Ono equation in  $H^s(\mathbb{R})$ . *International Mathematics Research Notices*, (2003), no. 26, 1449-1464.
- [26] D. Levy, C.-W. Shu and J. Yan. Local discontinuous Galerkin methods for nonlinear dispersive equations. *Journal of Computational Physics*, 196 (2004), no. 2, 751-772.
- [27] Y. Matsuno and D. J. Kaup. Initial value problem of the linearized Benjamin-Ono equation and its applications. *Journal of Mathematical Physics*, 38 (1997), no. 10, 5198-5224.
- [28] L. Molinet. Global well-posedness in  $L^2$  for the periodic Benjamin-Ono equation. *American Journal of Mathematics*, 130 (2008), no. 3, 635-683.
- [29] G. Ponce. On the global well-posedness of the Benjamin-Ono equation. *Differential and Integral Equations*, 4 (1991), 527-542.
- [30] W. H. Reed and T. R. Hill. Triangular mesh methods for the neutron transport equation. *Technical Report LA-UR-73-479*, Los Alamos Scientific Lab, 1973.
- [31] Z. Sun and C.-W. Shu. Error analysis of Runge-Kutta discontinuous Galerkin methods for linear time-dependent partial differential equations. *arXiv preprint [arXiv:2001.00971](https://arxiv.org/abs/2001.00971)*, (2020).
- [32] Z. Sun and C.-W. Shu. Strong stability of explicit Runge-Kutta time discretizations. *SIAM Journal on Numerical Analysis*, 57 (2019), no. 3, 1158-1182.
- [33] Z. Sun and C.-W. Shu. Stability of the fourth order Runge-Kutta method for time-dependent partial differential equations. *Annals of Mathematical Sciences and Applications*, 2 (2017), no. 2, 255-284.

- [34] T. Tao. Global well-posedness of the Benjamin-Ono equation in  $H^1(\mathbb{R})$ . *Journal of Hyperbolic Differential Equations*, 1 (2004), no. 1, 27-49.
- [35] V. Thomée and A. S. V. Murthy. A numerical method for the Benjamin-Ono equation. *BIT Numerical Mathematics*, 38 (1998), 597-611.
- [36] H. Wang, C.-W. Shu and Q. Zhang. Stability and error estimates of local discontinuous Galerkin methods with implicit-explicit time-marching for advection-diffusion problems. *SIAM Journal on Numerical Analysis*, 53 (2015), no. 1, 206-227.
- [37] H. Wang, C.-W. Shu and Q. Zhang. Stability analysis and error estimates of local discontinuous Galerkin methods with implicit-explicit time-marching for nonlinear convection-diffusion problems. *Applied Mathematics and Computation*, 273 (2016), 237-258.
- [38] Q. Xu and J. S. Hesthaven. Discontinuous Galerkin method for fractional convection-diffusion equations. *SIAM Journal on Numerical Analysis*, 52 (2014), no. 1, 405-423.
- [39] Y. Xu, Q. Zhang, C.-W. Shu and H. wang. The  $L^2$ -norm stability analysis of Runge-Kutta discontinuous Galerkin methods for linear hyperbolic equations. *SIAM Journal on Numerical Analysis*, 57 (2019), no. 4, 1574-1601.
- [40] Y. Xu and C.-W. Shu. Local discontinuous Galerkin methods for nonlinear Schrödinger equations. *Journal of Computational Physics*, 205 (2005), no. 1, 72-97.
- [41] Y. Xu and C.-W. Shu. Error estimates of the semi-discrete local discontinuous Galerkin method for nonlinear convection-diffusion and KdV equations. *Computer Methods in Applied Mechanics and Engineering*, 196 (2007), no. 37-40, 3805-3822.
- [42] Y. Xu and C.-W. Shu. Local discontinuous Galerkin methods for high-order time-dependent partial differential equations. *Communications in Computational Physics*, 7 (2010), no. 1, 1-46.
- [43] J. Yan and C.-W. Shu. A local discontinuous Galerkin method for KdV type equations. *SIAM Journal on Numerical Analysis*, 40 (2002), no. 2, 769-791.
- [44] Q. Zhang and C.-W. Shu. Error estimates to smooth solutions of Runge-Kutta discontinuous Galerkin methods for scalar conservation laws. *SIAM Journal on Numerical Analysis*, 42 (2004), no. 2, 641-666.